Neurobiology of Disease 127 (2019) 339–349

Contents lists available at ScienceDirect

Neurobiology of Disease

journal homepage: www.elsevier.com/locate/ynbdi

A mouse model of adult-onset multiple system atrophy

Kunikazu Tanji[a,*], Yasuo Miki[a], Fumiaki Mori[a], Yoshikazu Nikaido[b], Hidemi Narita[a,c], Akiyoshi Kakita[d], Hitoshi Takahashi[d], Koichi Wakabayashi[a]

[a] Department of Neuropathology, Institute of Brain Science, Hirosaki University Graduate School of Medicine, Hirosaki 036-8562, Japan
[b] Department of Anesthesiology, Hirosaki University Graduate School of Medicine, Hirosaki 036-8562, Japan
[c] Department of Rehabilitation Sciences, School of Health Sciences, Hirosaki University of Health and Welfare, Hirosaki 036-8102, Japan
[d] Department of Pathology, Brain Research Institute, University of Niigata, Niigata 951-8585, Japan

ARTICLE INFO

Keywords:
α-Synuclein
Cre-loxP technique
Model mouse
Multiple system atrophy
Oligodendrocyte
Phosphorylation

ABSTRACT

Multiple system atrophy (MSA) is an adult-onset neurodegenerative disorder clinically characterized by autonomic failure in addition to various combinations of symptoms of parkinsonism, cerebellar ataxia, and pyramidal dysfunction. Despite extensive research, the mechanisms underlying the progression of MSA remain unknown. Animal models of human diseases that recapitulate their clinical, biochemical and pathological features are indispensable for increasing our understanding of their underlying molecular mechanisms, which allows preclinical studies to be advanced. Because the onset of MSA occurs in middle age, an animal model that first manifests abnormal protein aggregates in adulthood would be most appropriate. We therefore used the Cre-loxP system to express inducible α-synuclein (Syn), a major component of the pathological hallmark of MSA, to generate a mouse model of MSA. Beginning in adulthood, these MSA model mice express excessive levels of Syn in oligodendrocytes, resulting in abnormal Syn accumulation and modifications similar to those observed in human MSA pathology. Additionally, MSA model mice exhibit some clinical features of MSA, including decreased motor activity. These findings suggest that this new mouse model of MSA represents a useful tool for analyzing the pathophysiological alterations that underlie the progression of this disease.

1. Introduction

Multiple system atrophy (MSA) is an adult-onset neurodegenerative disorder characterized by various degrees of symptoms of parkinsonism, cerebellar ataxia, and autonomic failure. Additionally, respiratory insufficiency and sudden death are clinical features observed in some MSA patients (Gilman et al., 2008). MSA was previously categorized into three diseases: striatonigral degeneration, olivopontocerebellar atrophy (OPCA) and Shy-Drager syndrome. Once pathological studies revealed that glial cytoplasmic inclusions (GCIs) were present in oligodendrocytes in all three of these diseases (Nakazato et al., 1990; Papp et al., 1989), patients with MSA were classified using a simplified system as either MSA-C (cerebellar ataxia) or MSA-P (parkinsonism) according to the relative predominance of clinical and pathological abnormalities (Gilman et al., 1999). Subsequent evidence has since demonstrated that α-synuclein (Syn) is a major component of both GCIs and Lewy bodies observed in Lewy body diseases, such as Parkinson's disease (PD) and dementia with Lewy bodies (DLB) ((Spillantini et al., 1998; Spillantini et al., 1997; Tu et al., 1998; Wakabayashi et al., 1997). These diseases are collectively referred to as α-synucleinopathies.

Based on these findings, several MSA models, in particular genetically modified MSA mouse models, have generated numerous mechanistic studies that have provided substantial contributions to what is currently known about MSA (Bassil et al., 2017; Kahle et al., 2002; Mandel et al., 2017; Shults et al., 2005; Yazawa et al., 2005). Relevant transgenic (Tg) and virus-based mouse models manifest MSA pathologies, such as GCIs, phosphorylated Syn deposits and abnormally aggregated Syn (Bassil et al., 2017; Mandel et al., 2017; Stefanova and Wenning, 2015). These MSA mouse models can also be analyzed to determine their biochemical properties, including Syn insolubility and oligomerization, which is observed in MSA patients. However, to induce the expression of Syn in MSA Tg mice, promoter activity is sustained during developmental stage. Therefore, Syn overexpression can cause latent developmental disturbance or compensatory effect within cells and tissues of these MSA mouse models. Furthermore, given that MSA is an adult-onset disease, it would be most ideal for Syn expression to increase in adulthood in model animals. To this end, we used the Cre-loxP system to create a new MSA model mouse. This technique enabled Syn expression to be induced in oligodendrocytes beginning in

* Corresponding author at: Department of Neuropathology, Institute of Brain Science, Hirosaki University Graduate School of Medicine, Hirosaki 036-8562, Japan.
E-mail address: kunikazu@hirosaki-u.ac.jp (K. Tanji).

https://doi.org/10.1016/j.nbd.2019.03.020
Received 23 August 2018; Received in revised form 20 March 2019; Accepted 21 March 2019
Available online 23 March 2019
0969-9961/

adulthood so that we could examine its effects on glial and neuronal degeneration.

We first generated mice harboring the first exon and the first intron of the chicken β-actin gene and a promoter (CAG promoter), followed by a loxP-flanked (flox) stop cassette-controlled Syn gene. After these mice were successfully generated, they were mated with mice in which Cre/estrogen receptor (ER) was specifically expressed under the proteolipid protein (plp) promoter in oligodendrocytes. When tamoxifen was injected, we confirmed that these MSA model mice exhibited numerous Syn inclusions in their oligodendrocytes in a manner resembling that of GCIs in human MSA patients. Further studies showed that these Syn inclusions were phosphorylated and resistant to proteinase K (PK) treatment. Importantly, these pathological findings preceded the manifestation of significant clinical abnormalities, including decreased motor activity.

2. Materials and methods

2.1. Generation of Syn knock-in mice, Syn-flox/flox

To generate a mouse model of MSA, we first generated Syn-flox mice that permitted the conditional induction of Syn protein. We cloned the Syn cDNA into a Rosa26 chicken β-actin (CAG) promoter-targeting vector for Cre/ER-mediated expression. According to previously described procedures (Soriano, 1999), a 5-kilobase (kb) fragment of Rosa26 was used to make the targeting constructs. This vector contained the following components: CAG - loxP- stop codons - three SV40 poly(A) sequences - loxP – the Syn gene - woodchuck hepatitis virus posttranscriptional regulatory element (WPRE) - bGH poly(A) - AttB - PGK promoter – FRT - Neomycin gene - PGK poly(A) - AttP (Fig. 1a. Ai3 vector, Addgene, Cambridge, MA) (Madisen et al., 2012). The final targeting vectors contained 5′ (1.1 kb) and 3′ homology (4.3 kb) arms as well as a PGK-DTA cassette for negative selection. The WPRE was used to enhance mRNA transcript stability (Gradinaru et al., 2008). The targeting vectors were linearized and transfected into the 129/B6 F1 hybrid embryonic stem (ES) cell line G4 using an Amaxa electroporator. G418-resistant ES clones were screened by using Southern blot analysis to probe *Avr*II-digested DNA with a 1.1-kb genomic fragment located immediately upstream of the 5′ arm. Positive ES cell clones were injected into C57BL/6 J blastocysts to obtain chimeric mice according to standard procedures. ES cell transfections and blastocyst injections were both performed by TransGenic Inc. (Kobe, Japan). Chimeric mice were bred with C57BL/6 J mice to achieve germline transmission. Germline transmission was confirmed by polymerase chain reaction (PCR) genotyping with the following primers: rosa F2731: 5'-CGA TGC TGG AAG GAT TGG AAC TAT GC-3′, and CAG R1: 5′-GAA ACA AGC CGT CAT TAA AC-3′. Fragments 4.3 kbp in size were amplified from Syn-flox mice. All animals were kept in temperature- and humidity-controlled rooms on a 12 h:12 h light:dark cycle in which the lights were on from 7:00 a.m. to 7:00 p.m. The mice were housed at 3–5 mice per cage with food and water provided ad libitum. All animal experiments in this study were performed in accordance with the Guidelines for Animal Experimentation and approved by the Animal Research Committee of Hirosaki University (approval number: M15044).

2.2. MSA model mice

The resulting Syn-flox mice were crossed with plp-Cre/ER mice, which are inducible Tg mice in which Cre is under the control of the human plp promoter and ER (Doerflinger et al., 2003). Breeding cages were maintained by mating Syn-flox/flox and Syn-flox/flox:plp-Cre/ER mice. Genotyping was done by PCR using primer sets binding to the Syn gene (*syn*-F12: 5'-CTG CAA CTC CAG TCT TTC-3′, syn-R11: 5'-CTG CAA CTC CAG TCT TTC-3′ and syn-R12: 5'-CTG CAA CTC CAG TCT TTC-3′). Fragments of 300 bp or 350 bp were amplified from Syn-flox mice or wild-type mice, respectively. Additionally, genotyping was done by PCR using primer sets binding to the Cre gene (CreERT-F1: 5′- GCG GTC TGG CAG TAA AAA CTA TC -3′, CreERT-R1: 5′- CTA GGC CAC AGA ATT GAA AGA TCT -3′ and CreERT-R2: 5′- GTA GGT GGA AAT TCT AGC ATC ATC C -3′). Fragments of 150 bp or 300 bp were amplified from plp-Cre/ER or wild-type mice, respectively. To excise the loxP sites via Cre recombination, adult mice (20 weeks old) were administered tamoxifen (100 mg/kg, intraperitoneally) once per day for five days. Tamoxifen (Sigma-Aldrich, Saint Louis, MO) was dissolved in corn oil at a final concentration of 10 mg/ml using a pestle and stored for up to 5 days at 4 °C in the dark. All control groups consisted of tamoxifen-injected control littermates.

2.3. Histopathological analyses

Mice were transcardially perfused with phosphate-buffered saline (PBS). The brain and spinal cord were removed, and the left hemisphere was frozen at −80 °C for subsequent biochemical analyses. The right hemisphere was fixed in 4% paraformaldehyde for 48 h. After the tissues were dehydrated through a graded series of ethanol solutions, they were embedded in paraffin, cut into 4-μm-thick sections and stained with hematoxylin and eosin or underwent Klüver-Barrera (KB) staining.

Tissue sections were heated in an autoclave for 15 min in 10 mM citrate buffer (pH 6.0) for antigen retrieval. Some sections were then incubated with PK (Gibco BRL, Gaithersburg, MD; 50 μg/ml) in PK buffer (10 mM Tris-HCl, pH 7.8; 100 mM NaCl, 0.1% and Nonidet-P40) at 37 °C for 5 min to detect PK-resistant Syn. The sections were then subjected to immunohistochemical staining using the avidin-biotin-peroxidase complex method. Diaminobenzidine (DAB) was used as the chromogen. The sections were counterstained with hematoxylin. To detect phosphorylated Syn in neuronal cells, DAB and alkaline phosphatase substrate Kit III (Vector, Burlingame, CA) were used as the chromogens.

Double-immunofluorescence staining was performed to detect the coexpression of phosphorylated Syn and either glial fibrillary acidic protein (GFAP; IBL, Gunma, Japan; 1:1000) or myelin basic protein (MBP; LSBio, Seattle, WA; 1:250). Deparaffinized sections were blocked in goat and horse sera and then incubated overnight at 4 °C in a mixture of polyclonal anti-GFAP or -MBP and monoclonal anti-phosphorylated Syn (1:2000) antibodies. After the sections were washed 3 times for 5 min each with PBS, they were incubated for 1 h with Alexa Fluor 488- and 594-conjugated secondary antibodies (Invitrogen). After they were rinsed in PBS, the sections were mounted with ProLong Gold Antifade Reagent containing 4′,6-diamidino-2-phenylindole (DAPI; Invitrogen) and examined using a confocal microscope (EZ-Ci, Nikon, Tokyo, Japan). Adobe Photoshop CS5 software (Adobe systems, San Jose, CA) was used for image processing. Electron microscopy analysis and information on the antibodies we used are described in the supplemental materials and methods section.

2.4. Biochemical analyses

Southern blot analysis, PCR, sample preparation and Western blot analysis are described in the supplemental Materials and methods section.

2.5. Behavioral analyses

Several kinds of behavioral analyses are described in the supplemental Materials and methods section.

2.6. Quantitative and statistical analysis

The percentage of cell numbers were quantified from three Tg or control mice at indicated postnatal days. (Two slides from each mice). Digital images were captured with a microscope (BX 63, Olympus, Tokyo, Japan) with a digital camera (DP80, Olympus). For cell

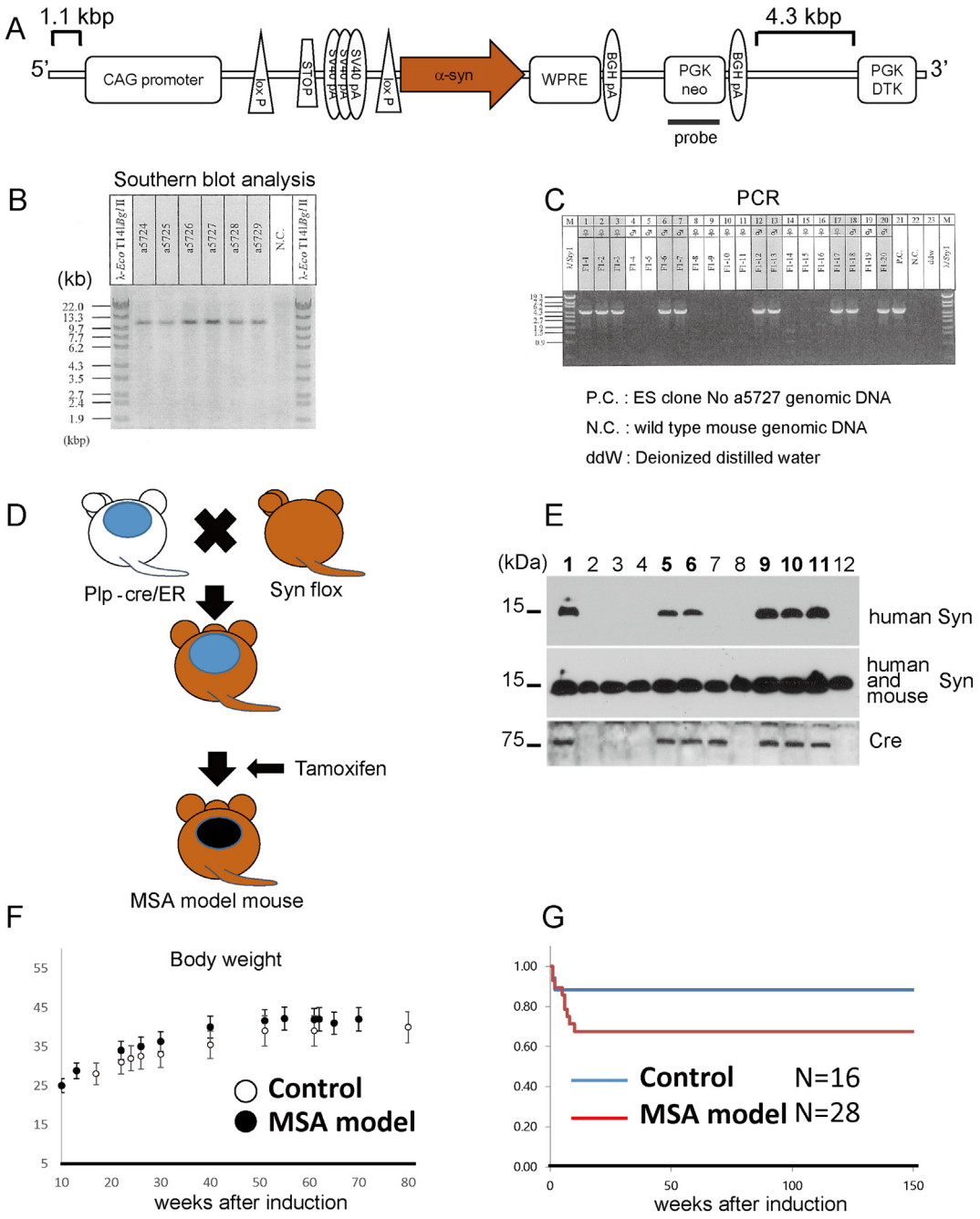

Fig. 1. Generation of Syn-flox and Syn-plp mice. (A) Schematic diagram of the gene targeting cassette inserted into the Rosa26 locus. To generate GAG-Syn-flox transgenic (Tg) mice harboring a transgene containing loxP-stop-loxP-Syn under the CAG promoter, the gene targeting cassette was linearized and inserted into ES cells. (B) G418 antibiotic-resistant ES clones were screened by Southern blot analysis using *Avr*II-digested genomic DNA with the probes indicated in A. (C) PCR was used to genotype the mice. (D) Strategy for generating MSA model mice. To generate mice that expressed Syn specifically in oligodendrocytes, CAG-Syn-flox/flox mice were mated with plp-Cre/ER mice. To activate Cre-mediated recombination in oligodendrocytes, tamoxifen (100 mg/kg, i.p.) was injected for 5 consecutive days. (E) Protein was extracted from mice after Syn induction. Western blot analysis performed using human-specific antibodies against Syn confirmed that Syn was robustly expressed in mice harboring both the Cre and Syn genes (1, 5, 6, 9, 10, and 11 in number) but not in those with either Cre or Syn. (F) The body weights of MSA model (black circle) and control (white circle) mice are shown (mean +/− SD, $n = 10$ per group). The mice exhibited no apparent abnormalities in feeding behavior, sexual behavior and body weight. (G) Kaplan-Meier tests indicating the survival rates in MSA model and control mice.

counting, three to five areas were randomly selected according to a predesigned zig-zag pattern and we counted the number of cells that stained positively for NeuN (mouse anti-NeuN Antibody, clone A60, Millipore, Bedford, MA) as neuron. The counting frame width (X) and height (Y) was 0.25 mm producing a counting frame area (XY) of 0.0625 mm^2. For neuron in the cerebellar granule layer, KB stain was also used for cell counting, because it sometimes was hard to distinguish each neuron. Similarly, we counted the number of cells expressing GFAP, or IbaI (Wako, Osaka, Japan; 1:500) as astrocytes or microglia, respectively. Cell number were normalized by that in means of control samples, and indicated as mean + SD. The control value was defined as 1.0. Statistical significance was evaluated using one-way ANOVA with Bonferroni's post hoc test for 3 or more groups and Student's *t*-test for two groups. For motor performance tests, repeated ANOVA was used.

A semiquantitative analysis of protein levels was performed using

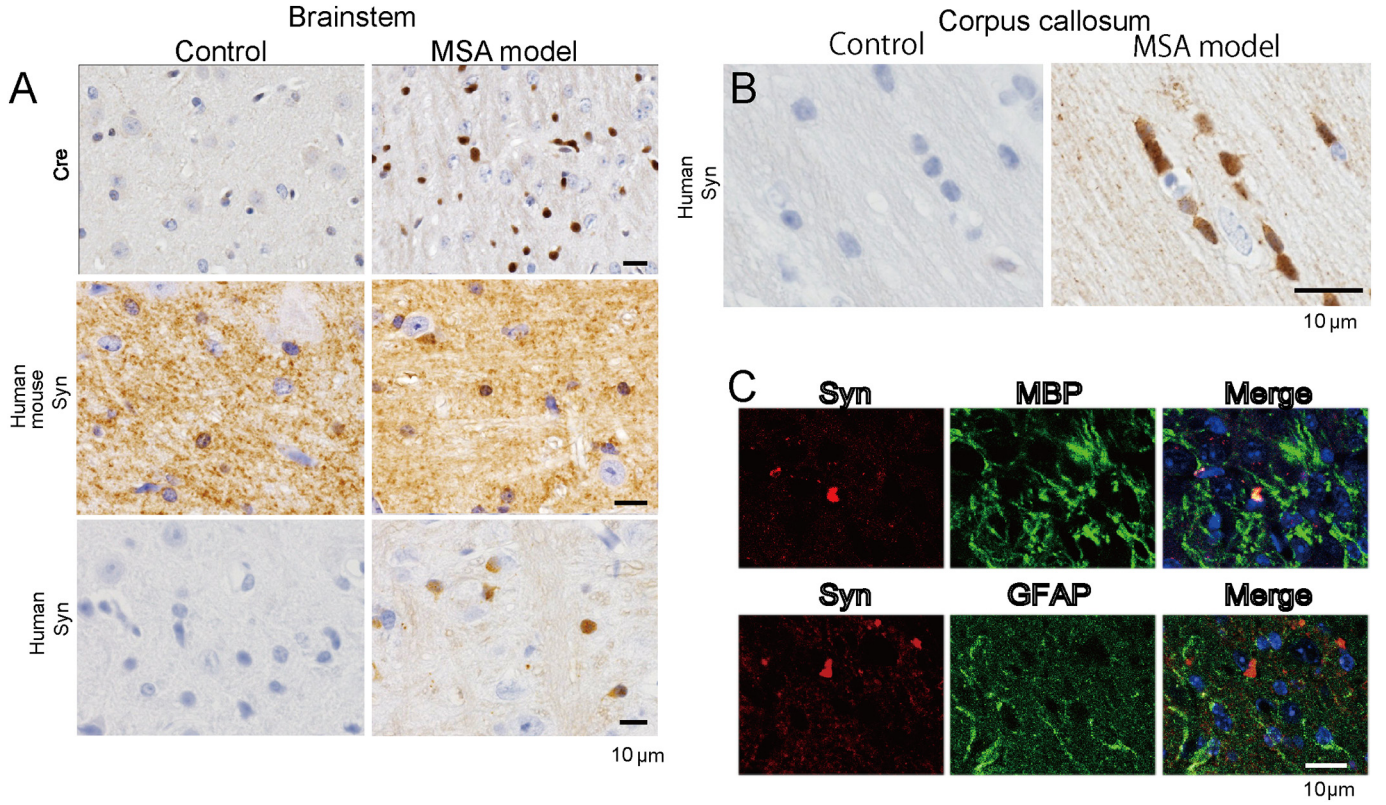

Fig. 2. Confirmation of MSA model mice. (A, B) Immunohistochemical study showing that Cre expression was observed only in the Syn-plp mice (MSA model mice) treated with tamoxifen (24-week-old mice). An antibody against both mouse and human Syn reacted equally with tissues obtained from control and MSA model mice, whereas an antibody specific to human Syn immunostained glial cells only in the brainstem (A) and corpus callosum (B) in MSA model mice. (C) Double immunofluorescence performed using antibodies against Syn and either GFAP or MBP. In MSA model mice, there was significant overlap in Syn and MBP expression in the white matter.

ImageJ software provided by the National Institutes of Health (NIH). All data were shown as the mean ± standard deviation (SD). Chi-square analysis was performed to determine the survival rate. A probability value of < 0.05 ($p < .05$) was considered to indicate significance.

3. Results

3.1. Generation of a new MSA mouse model

We generated MSA model mice in two steps. Initially, we generated a gene-targeting line of Syn-loxP mice in which the CAG - promoter - loxP - STOP - loxP - Syn gene cassette was knocked into the ROSA26 locus (Fig. 1A). Rosa26 is a ubiquitously expressed locus into which an exogenous strong promoter can be inserted to drive higher expression of a target gene (Muzumdar et al., 2007; Soriano, 1999; Zong et al., 2005). We identified several ES cells positive for the neo probe and the 5′ and 3′ probes according to southern blotting analysis (Fig. 1B, Supplementary Fig. 1) and PCR (Fig. 1C). We inserted the positive ES cells into C57BL/6 J blastocysts to obtain chimeric mice and successfully generated Syn-flox mice via germ-line transmission. These mice were then mated with plp-Cre/ER mice (Fig. 1D), in which Cre/ER is specifically expressed in oligodendrocytes under the control of the plp promoter (Doerflinger et al., 2003).

Alternatively, to confirm Cre-recombinase activity in the plp-Cre/ER mice, we generated plp-Cre/ER:flox-LacZ mice by mating plp-Cre/ER mice with RNZ mice (Kobayashi et al., 2013). Consistent with previous findings (Doerflinger et al., 2003), β-galactosidase staining showed that LacZ was readily detected in glial cells only after tamoxifen was injected (Supplementary Fig. 2), indicating that the plp-Cre/ER mice were suitable for our purposes.

After we mated Syn-flox mice with plp-Cre/ER mice, the mice were born at the expected normal Mendelian ratios (Syn-plp mice) and were visually indistinguishable from control mice. To induce Cre recombinase activity, tamoxifen was administered to adult Syn-plp mice (20-weeks old). Western blot analyses performed using a specific antibody against human Syn showed that Syn was clearly induced in the brains of the Syn-plp mice (Fig. 1E), whereas no positive staining was observed in the controls (Syn-flox/flox with or without tamoxifen and Syn-plp without tamoxifen). The Syn-plp mice treated with tamoxifen are hereafter called ‘MSA model mice’. There was no significant difference in body weight between the MSA and control mice after tamoxifen induction (Fig. 1F). We noticed that after Syn induction, the rate of sudden death was relatively higher in male MSA model mice than in male controls (Fig. 1G). When mice with sudden death were excluded, life span did not differ between the remaining MSA model mice and the controls until 2 years after induction.

3.2. Syn inclusions are mainly aggregated in oligodendrocytes

Immunostaining using an antibody against human Syn indicated that at 1 week after Syn induction, the MSA model mice expressed human Syn predominantly in glial cells (Fig. 2A, B). To determine whether Syn expression was localized in oligodendrocytes or astrocytes, sections were reacted with antibodies against phosphorylated Syn and MBP or GFAP, respectively. Double immunofluorescent staining demonstrated that human Syn expression was found in MBP-labeled glial cells, indicating that Syn-positive signals were oligodendrocyte specific (Fig. 2C). Immunoelectron microscopy revealed that human Syn-positive immunoproducts were detected on the membranes of intranuclear

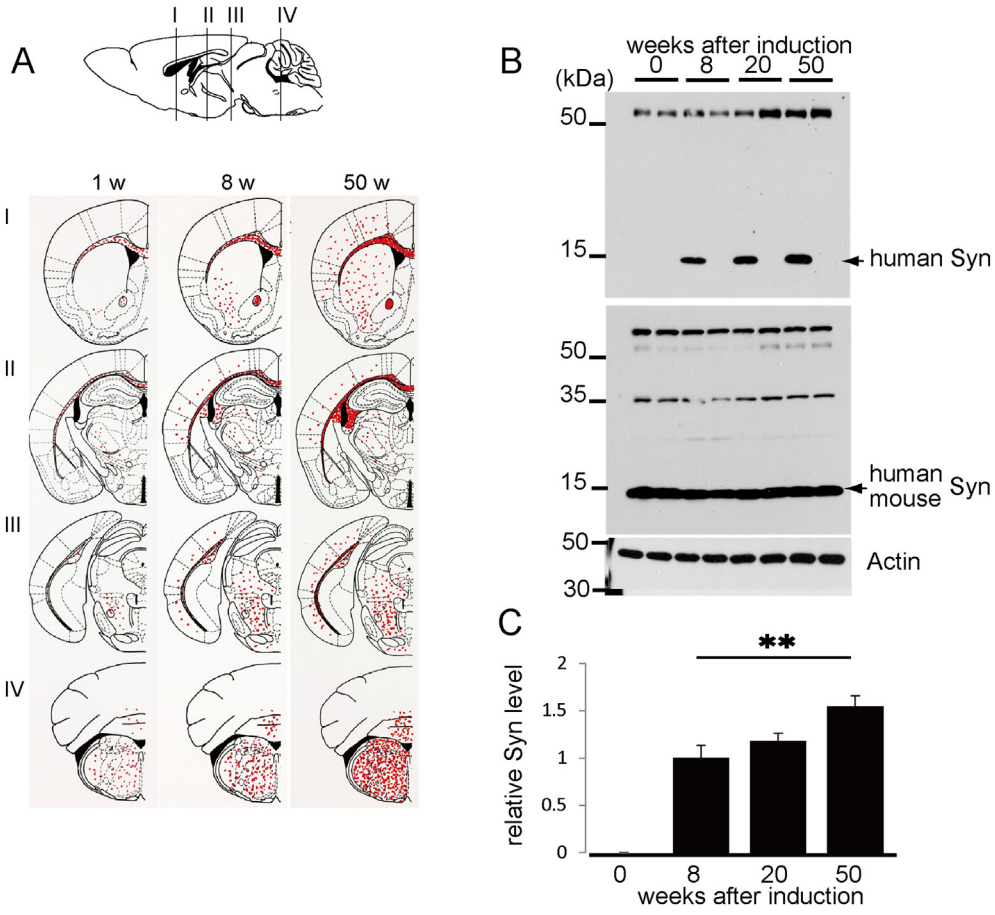

Fig. 3. Syn expression gradually spread throughout the central nervous system, mainly in the white matter of MSA model mice. (A) Schematic distribution of human Syn deposits. Human Syn aggregated in the brainstem and cerebellum of MSA model mice at 1, 8 and 50 weeks after Syn induction. Red labeling indicates Syn aggregates. (B) Syn expression was examined by immunoblotting, and the results indicated that at 8, 20, and 50 weeks after Syn induction, human Syn was robustly expressed in MSA model mice but not in controls. (C) Quantitative data for the experiments shown in B. (For interpretation of the references to colour in this figure legend, the reader is referred to the web version of this article.)

vesicular structures in the nuclei of oligodendrocytes located in the corpus callosum of the MSA model mice (Supplementary Fig. 3C, F) but not the Cre-LacZ mice (Supplementary Fig. 3A, D) or the Syn-flox mice (Supplementary Fig. 3B, E). To further demonstrate that Syn expression expanded with age, we analyzed the distribution of human Syn in the brains of MSA model mice at 1, 8, and 50 weeks after Syn induction and found that Syn expression gradually spread throughout the central nervous system, mainly in the white matter (Fig. 3A). Syn was also expressed in oligodendrocytes in the gray and white matter of the spinal cords of MSA model mice (Supplementary Fig. 4). Syn expression levels gradually increased by approximately 1.5-fold in MSA model mice treated for a longer period after induction than in those treated for a shorter period (Fig. 3B, C).

In MSA patients, Syn expression in oligodendrocytes is abnormally modified by phosphorylation and becomes resistant to PK treatment. Our immunohistochemical studies revealed that human Syn was clearly phosphorylated at S129, similar to that observed in MSA pathology, although the 4D6 antibody reacted equally with Syn in the control and MSA model mice (Fig. 4A-F). Furthermore, PK-resistant Syn appeared in the white matter of MSA model mice for longer periods after Syn induction (Fig. 4G, H). Glial inclusions in oligodendrocytes of MSA model mice were also immunostained with the 5G4 antibody, which is reported to bind specifically to the Syn oligomer and disease-associated Syn (Kovacs et al., 2014; Kovacs et al., 2012) (Fig. 4I, J).

3.3. MSA model mice exhibit lower levels of spontaneous activity

We performed several behavioral analyses to examine the effects of Syn induction on behavioral phenotypes. There was no significant difference in performance in an open field test at 4 weeks after Syn induction, whereas at 20 and 50 weeks after induction, significant deterioration was observed in the MSA group, which had a shorter moving distance (Fig. 5A). In rotarod tests, there were significant deficits in motor coordination and balance in the MSA model mice at longer time points after Syn induction (Fig. 5B and Supplementary movie). We initially assumed that the lower motor activity was attributable to a depressive-like phenotype. To investigate this possibility, we performed a forced swimming test, and the results indicated that there was no difference in immobility between the MSA model mice and controls (Fig. 5C). Thus, the lower activity observed in the rotarod tests may not be due to a depressive-like phenotype in the MSA model mice. No muscle abnormalities were detected in the MSA model mice upon gross and histological examinations of the upper and lower extremities (Supplementary Fig. 5). Accordingly, there was no difference in grip handling performance between the MSA model and control mice (Fig. 5D).

3.4. Neuronal pathology progresses in the early stage after Syn induction

We could not find neuronal loss in the anterior horn and certain regions corresponding to human MSA lesions: the cerebellum, brainstem, substantia nigra and striatum (Figs. 6A and B, Supplementary Figs. 6 and 7). Nevertheless, we found that in MSA model mice 1 week after Syn induction, Syn was deposited in the perinuclear area in certain neurons and especially in neurons located in the brainstem and putamen, where MAP1B-positive cells contained phosphorylated Syn (Fig. 6D). several reports showed that perinuclear Syn inclusions were found in the central nervous system of MSA patients during the preclinical stage (Fig. 6C) (Fujishiro et al., 2008; Kon et al., 2013; Parkkinen et al., 2007; Rodriguez-Diehl et al., 2012). Furthermore, GFAP-positive or IbaI-positive signals were more intense in MSA model mice examined at later time points after Syn induction (Fig. 6E, F and

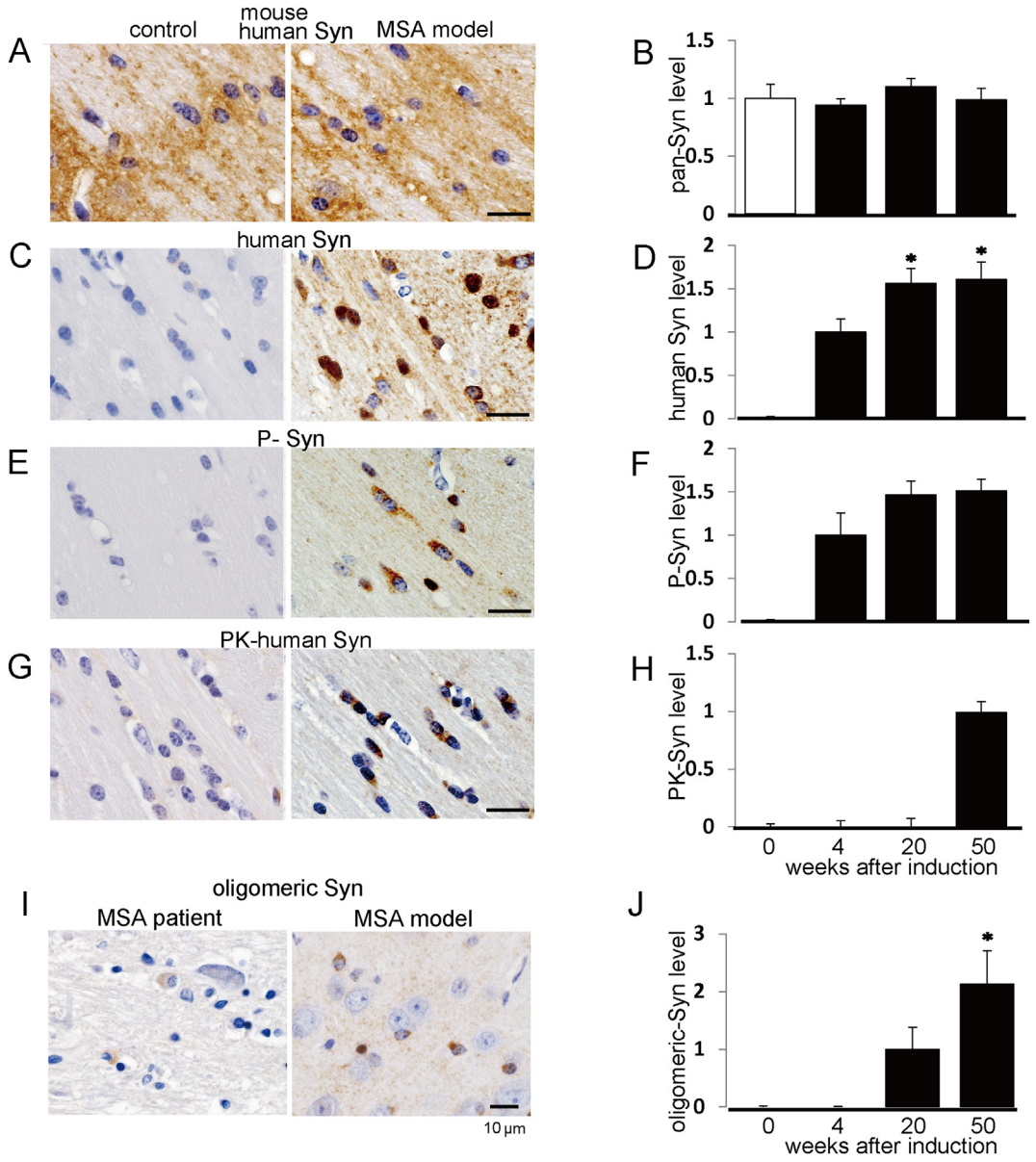

Fig. 4. MSA model mice exhibit pathological abnormality of Syn. (A, B) Immunohistochemical staining of tissue sections of cerebral white matter obtained from mice after tamoxifen induction. (A, B) There was no difference in the 4D6 antibody staining pattern between the 24-week-old control and MSA model mice. (C, D) The LB509 antibody reacted with GCIs in the 24-week-old MSA model but not control mice. (E, F) Phosphorylated Syn was observed in the 24-week-old MSA model mice. (G, H) PK-resistant Syn appeared in the 70-week-old MSA model mice. (I) Immunohistochemical staining of tissue sections of cerebral white matter obtained from MSA patients and 40-week-old MSA model mice after tamoxifen induction. An antibody against oligomeric Syn (5G4) reacted with GCIs in patient with MSA (left). The 5G4 antibody recognized glial inclusions in MSA model mice (right). (J) Quantitative data for oligomeric Syn expression of MSA model mice with age.

Supplementary Fig. 8). Ubiquitin accumulation is one of the hallmarks of neurodegenerative disorders. Unexpectedly, we found that ubiquitin-positive staining was localized not only in glial cells but also in neurons (Fig. 6G). Ubiquitin-positive structures were positively labeled with a K48- or K63-lined ubiquitin antibody (Supplementary Fig. 9), suggesting that proteostasis and cellular signaling were gradually disrupted in these neurons.

3.5. Phosphorylated Syn is detected in higher-density fractions

We previously demonstrated that abnormal Syn was detected in higher-density fractions of DLB (Tanji et al., 2010). Like abnormal Syn extracted in DLB, a filter-trap assay showed that an antibody against phosphorylated Syn recognized lysates in higher-density fractions in MSA tissues (arrowhead in Fig. 7A, B) but not in controls. Similarly, lysates in the higher-density fractions of MSA model mice were also labeled by an antibody for phosphorylated Syn (Fig. 7C, D). It was previously reported that Syn becomes an insoluble protein in MSA patients (Tu et al., 1998). Sequential biochemical fractionation demonstrated that the LB509 antibody recognized proteins in Triton X-100-insoluble (III) and -soluble fractions (I and II) in the MSA model mice (Fig. 7E, F, and G). Collectively, these results indicate that the Syn protein is abnormally modified in MSA model mice, in which some of the properties of MSA patients are replicated.

4. Discussion

MSA is an adult-onset synucleinopathy that is currently incurable. Preclinical animal models of MSA are needed for studies aimed at identifying the mechanisms underlying and medications to prevent and

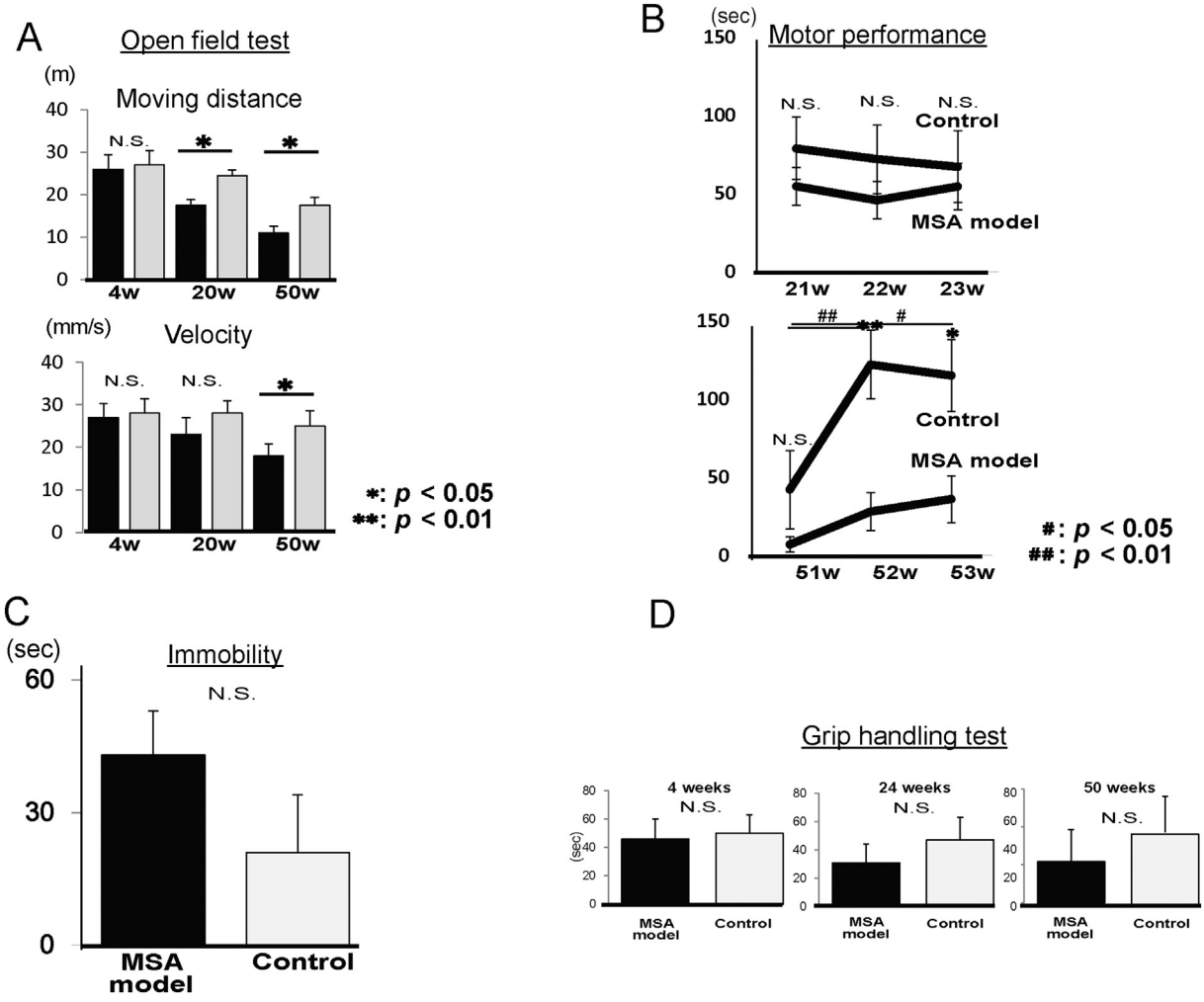

Fig. 5. MSA model mice exhibit lower motor performance and activity. (A) Open field tests revealed that MSA model mice displayed repressed motor activity as indicated by moving distance and velocity. (B) Twenty- or fifty-week-old mice successfully performed the rotarod task and achieved a stable level of performance within 3 days of beginning training when tested at a constant speed of 4 rpm. Repeated two way ANOVA shows that a significant effect of genotype and age in rotarod test in fifty-week-old MSA model mice (effect of genotype $F_{1,\ 32} = 5.903$, $p = .0112$, effect of age $F_{2,\ 32} = 13.949$, $p = .0013$, interaction, $F_{2,\ 32} = 11.886$, $p = .0073$,). Post hoc Bonferroni correction indicates decrease of sustained time in MSA model mice at 52- and 53- weeks of age compared with control.* $p < .05$, ** $p < .01$,versus age-matched control; # $p < .05$, ## $p < .01$, for all groups. There were no difference between twenty-week-old MSA model and control mice. (C) Forced swimming tests showed that there was no significant difference in immobile time between the MSA model and control mice. (D) Grip handling tests indicated that there was no difference in grip power between the MSA model and control mice. Error bars show the standard deviations. Three types of controls were used for survival and behavioral tests: Cre alone, Syn alone, and Syn-flox/flox without tamoxifen injection.

treat this disease. To this end, we generated two lines of genetically modified mice: Syn-loxP and Syn-plp mice. In particular, the latter can be used as an MSA model after tamoxifen injection, which initiates Cre recombinase activity. Because MSA is an adult-onset disease, we aimed to examine the effects of Syn expression on MSA pathophysiology in adult or later stages. As expected, we observed robust expression of Syn, which exhibited several abnormal modifications, in the MSA model mice. We used the Cre-LoxP method to temporally control Syn expression in oligodendrocytes, and tamoxifen was used to induce Cre nuclear translocation (Feil et al., 1996). The Plp promoter was utilized to express Cre specifically in oligodendrocytes, in which it induced the deletion of stop codons located upstream of the Syn cDNA, resulting in robust Syn expression. Although a substantial number of papers have supported the safety of tamoxifen, it does cause some damage to the body. Therefore, in this study, for all MSA-control comparisons, the control mice were also injected with tamoxifen. We unexpectedly found that after Syn induction, approximately 30% of the male MSA model mice exhibited sudden death, and this rate was much higher than that observed in the tamoxifen-treated controls.

Sudden death is one of the causes of death in human MSA patients (Gilman et al., 2008). However, we think that the cause of sudden death in MSA model mice is different from that in MSA patients. In most MSA patients, sudden death tends to happen during the advanced stage (Gilman et al., 2008), whereas it happened just a few days after tamoxifen injection in MSA model mice. Furthermore, a large-scale survey of MSA patients in several clinical studies indicated that there was no difference in the rate of sudden death between male and female MSA patients (Wenning et al., 2013; Zhang et al., 2018). Although we have no clear answer why sudden death occurred predominantly at the early stage in MSA model mice, we hypothesize that a tamoxifen-induced surge in Syn expression may contribute to the disturbance of neurotransmitter release, resulting in the sudden death observed in MSA model mice, because Syn is a presynaptic protein that regulates neurotransmitter release (Kalia and Lang, 2015). Further studies will be needed to clarify the mechanism of sudden death observed in MSA model mice.

Importantly, no obvious symptoms were observed in the MSA model mice during the early period following induction (< 4 weeks after Syn

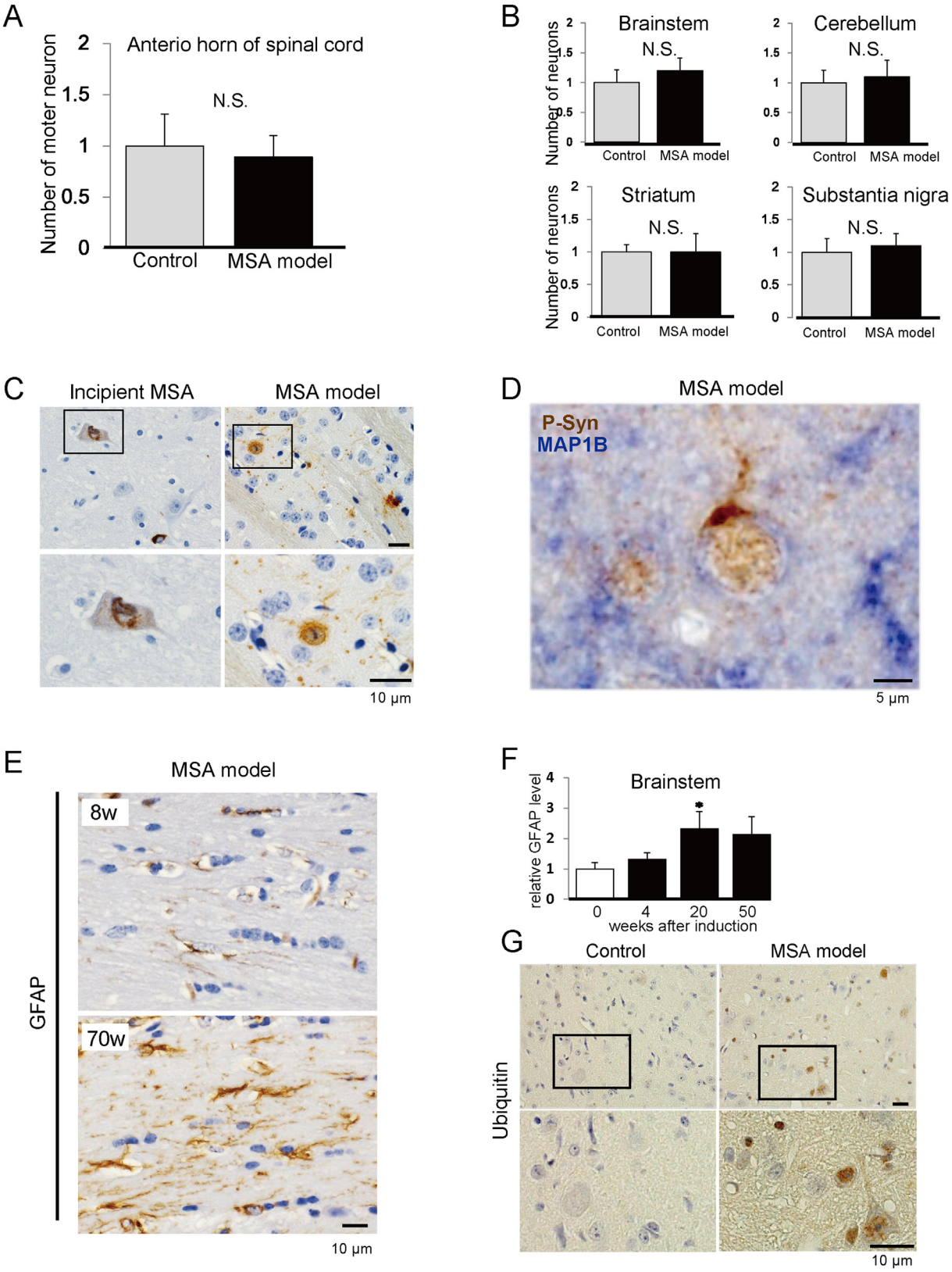

Fig. 6. Pathological changes in the early phase in MSA model mice. (A) Quantitative analysis showing that any neuronal loss was found in the anterior horn of spinal cord of MSA model mice. (B) Quantitative analysis showing that any neuronal loss was found in the brainstem, cerebellum, striatum and substantia nigra of MSA model mice. (C) Perinuclear Syn was observed in neurons and GCI-containing oligodendrocytes in incipient MSA patients. Abnormal Syn was observed in the perinuclear area of neurons located in the putamen and brainstem of 21-week-old MSA model mice after Syn induction (1 week after Syn induction). (D) Double immunostaining with a neuronal marker, (microtubule-associated protein 1B; MAP1B) and phosphorylated Syn shows that P-Syn-positive structure are located in MAP1B-labeled cells. (E) The inflammatory response substantially accelerated with age. (F) Quantitative data for GFAP-positive structures in MSA model mice. (G) Ubiquitin-positive staining was observed in glial and neuronal cells of MSA model mice (24 weeks old). Bars = 10 μm (C, E, G) and 5 μm (D).

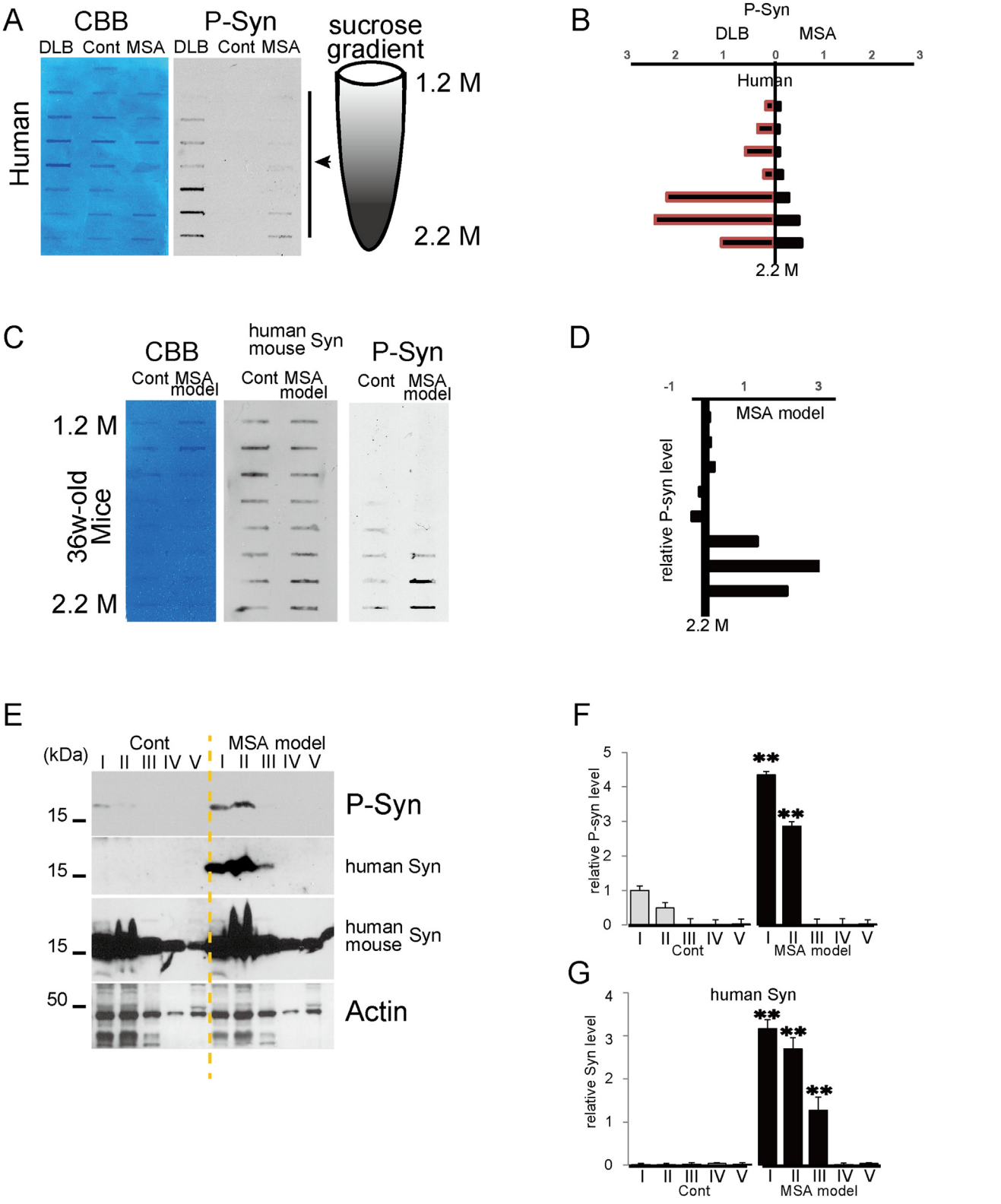

Fig. 7. Biochemical features in MSA model mice and patients.

induction). However, pathological and biochemical studies clearly demonstrated that numerous GCI and neuronal cytoplasmic and nuclear inclusions were present during this period. Considering that several groups have also reported the occurrence of perinuclear Syn accumulation in neurons in incipient MSA patients (Fujishiro et al., 2008; Kon et al., 2013), it is worth noting that abnormal Syn was observed in the neuronal perinuclear area of certain regions, such as the putamen and brainstem, of MSA model mice at short durations (< 4 weeks) after Syn induction. This finding raises two possibilities: that neuronal Syn is ectopically expressed in neuronal cells or transferred from oligodendrocytes. Since several papers reported that PLP gene expresses in the neurons of the medulla, olfactory bulb and cerebellum of mice during

relative early postnatal days (< 14 days, Bongarzone et al., 1999; Michalski et al., 2011; Miller et al.,2008), we should carefully raise the latter possibility with more pathological and biochemical data in the future. Collectively, these data indicate that our MSA model mice can offer the possibility to clarify the molecular mechanisms underlying the preclinical stages of this disease.

At longer time points after Syn induction, the MSA model mice exhibited some clinical features of MSA, including decreased motor activity. Sucrose gradient analysis showed that the density of Syn was higher in the MSA model mice, similar to that found in tissues obtained from MSA patients. Furthermore, Syn was extracted from the Triton X-100-insoluble fraction in MSA model mice. In agreement with these biochemical findings, we also found that PK-resistant Syn appeared in the MSA model mice at longer time points after Syn induction. Phosphorylated and oligomeric Syn were also evident in the MSA model mice. Moreover, immunostaining for astrocytes and microglia revealed that the inflammatory response as sustained in MSA model mice examined at longer time points after Syn induction. Additionally, ubiquitin immunohistochemistry showed that ubiquitin had clearly accumulated not only in the GCIs but also in some neuronal cytoplasmic and nuclear inclusions of the MSA model mice. Interestingly, we found no abnormal Syn deposits in the neurons exhibiting ubiquitin accumulation. Ubiquitin functions as a tag for protein degradation and a modulator of cell signaling. Immunostaining showed that some neurons without Syn deposits were both K48-linked and K63-linked ubiquitin-immunopositive. Given that ubiquitin accumulation is a common hallmark of neurodegenerative diseases, these data suggest that proteostasis was gradually disrupted in these neurons.

We cannot find any pathological evidence showing neuronal loss in any regions. However, KB staining showed relatively weaker myelin staining in the white matter of spinal cord of MSA model mice than that in controls. Taken together with findings that abnormal ubiquitin deposited in some neurons, axonal flow and/or neural dysfunction may occur in MSA model mice. Thus, we hypothesize that gradual disturbances in physiological neuronal and glial activities contributed to the lower levels of motor activity observed in the MSA model mice.

In conclusion, we generated Tg mice in which human Syn expression was induced in adulthood and confirmed that human Syn was expressed in oligodendrocytes in certain regions of the mouse brain. The MSA model mice replicate some pathological, biochemical and clinical features of MSA patients, indicating that Syn accumulation in oligodendrocytes results in neuronal dysfunction and may be associated with the mechanisms underlying MSA. Earlier treatment is important for slowing MSA. Our MSA model offers a unique approach to advancing our understanding of the mechanisms underlying the initial disease progression and developing novel therapeutics for MSA.

Supplementary data to this article can be found online at https://doi.org/10.1016/j.nbd.2019.03.020.

Disclosure

K.T. and K.W. are applying for a patent for Syn-plp to enable its use as an MSA model following tamoxifen administration, as described here (patent application number: PA-16-16).

(A) Filter-trap assay showing that a higher density of Syn was phosphorylated in MSA patients. DLB was used as a positive control for phosphorylated Syn. Coomassie blue staining indicating that almost equal amounts of protein were applied in the DLB, control and MSA samples. Arrowhead indicates phosphoryalted Syn in a MSA patient. (B) Quantitative analysis of the data shown in A. Compared with the controls, the MSA samples contained relatively higher levels of phosphorylated Syn levels, especially in higher-density fractions. (C) Phosphorylated Syn was also extracted from fractions with higher densities in MSA model mice (36 weeks old). (D) Quantitative analysis of the data shown in C. The relative levels of phosphorylated Syn were measured. (E) Sequential fractionation revealed phosphorylated Syn in Triton X-100-soluble fractions of tissues obtained from 36-week-old MSA model mice. Actin was used as a loading control. The methods used to prepare the samples obtained from fractions I, II, III, IV, and V are described in detail in the Materials and methods section. (F) The value of the control mice (lane I) was defined as 1-fold when determining the immunoreactive densities of phosphorylated Syn. (G) Quantitative analysis of the data shown in E regarding human Syn. (For interpretation of the references to color in this figure legend, the reader is referred to the web version of this article.)

Acknowledgements

This work was supported by JSPS KAKENHI grant numbers 17K07089 (K.T.), 16K15473 (Y.M.), 17K07088 (F.M.), and 18H02533 (K.W.); the Hirosaki University Institutional Research Grant (K.T., and K.W.); and The Collaborative Research Project (2018-2810) of the Brain Research Institute, Niigata University. The authors wish to express their gratitude to Dr. Itohara for generously providing us the RNZ mice (ROSA-loxP-STOP-loxP-nls-LacZ) from RIKEN and to M. Nakata and A. Ono for their technical assistance.

References

Bassil, F., Guerin, P.A., Dutheil, N., Li, Q., Klugmann, M., Meissner, W.G., Bezard, E., Fernagut, P.O., 2017. Viral-mediated oligodendroglial alpha-synuclein expression models multiple system atrophy. Mov. Disord. 32, 1230–1239.

Bongarzone, E.R., Campagnoni, C.W., Kampf, K., Jacobs, E.C., Handley, V.W., Schonmann, V., Campagnoni, A.T., 1999. Identification of a new exon in the myelin proteolipid protein gene encoding novel protein isoforms that are restricted to the somata of oligodendrocytes and neurons. J. Neurosci. 19, 8349–8357.

Doerflinger, N.H., Macklin, W.B., Popko, B., 2003. Inducible site-specific recombination in myelinating cells. Genesis. 35, 63–72.

Feil, R., Brocard, J., Mascrez, B., LeMeur, M., Metzger, D., Chambon, P., 1996. Ligand-activated site-specific recombination in mice. Proc. Natl. Acad. Sci. U. S. A. 93, 10887–10890.

Fujishiro, H., Ahn, T.B., Frigerio, R., DelleDonne, A., Josephs, K.A., Parisi, J.E., Eric Ahlskog, J., Dickson, D.W., 2008. Glial cytoplasmic inclusions in neurologically normal elderly: prodromal multiple system atrophy? Acta Neuropathol. 116, 269–275.

Gilman, S., Low, P.A., Quinn, N., Albanese, A., Ben-Shlomo, Y., Fowler, C.J., Kaufman, H., Klockgether, T., Lang, A.E., Lantos, P.L., Litvan, I., Mathias, C.J., Oliver, E., Robertson, D., Schatz, I., Wenning, G.K., 1999. Consensus statement on the diagnosis of multiple system atrophy. J. Neurol. Sci. 163, 94–98.

Gilman, S., Wenning, G.K., Low, P.A., Brooks, D.J., Mathias, C.J., Trojanowski, J.Q., Wood, N.W., Colosimo, C., Durr, A., Fowler, C.J., Kaufmann, H., Klockgether, T., Lees, A., Poewe, W., Quinn, N., Revesz, T., Robertson, D., Sandroni, P., Seppi, K., Vidailhet, M., 2008. Second consensus statement on the diagnosis of multiple system atrophy. Neurology. 71, 670–676.

Gradinaru, V., Thompson, K.R., Deisseroth, K., 2008. eNpHR: a Natronomonas halorhodopsin enhanced for optogenetic applications. Brain Cell Biol. 36, 129–139.

Kahle, P.J., Neumann, M., Ozmen, L., Muller, V., Jacobsen, H., Spooren, W., Fuss, B., Mallon, B., Macklin, W.B., Fujiwara, H., Hasegawa, M., Iwatsubo, T., Kretzschmar, H.A., Haass, C., 2002. Hyperphosphorylation and insolubility of alpha-synuclein in transgenic mouse oligodendrocytes. EMBO Rep. 3, 583–588.

Kalia, L.V., Lang, A.E., 2015. Parkinson's disease. Lancet. 386, 896–912.

Kobayashi, Y., Sano, Y., Vannoni, E., Goto, H., Suzuki, H., Oba, A., Kawasaki, H., Kanba, S., Lipp, H.P., Murphy, N.P., Wolfer, D.P., Itohara, S., 2013. Genetic dissection of medial habenula-interpeduncular nucleus pathway function in mice. Front. Behav. Neurosci. 7, 17.

Kon, T., Mori, F., Tanji, K., Miki, Y., Wakabayashi, K., 2013. An autopsy case of preclinical multiple system atrophy (MSA-C). Neuropathology. 33, 667–672.

Kovacs, G.G., Wagner, U., Dumont, B., Pikkarainen, M., Osman, A.A., Streichenberger, N., Leisser, I., Verchere, J., Baron, T., Alafuzoff, I., Budka, H., Perret-Liaudet, A., Lachmann, I., 2012. An antibody with high reactivity for disease-associated alpha-synuclein reveals extensive brain pathology. Acta Neuropathol. 124, 37–50.

Kovacs, G.G., Breydo, L., Green, R., Kis, V., Puska, G., Lorincz, P., Perju-Dumbrava, L., Giera, R., Pirker, W., Lutz, M., Lachmann, I., Budka, H., Uversky, V.N., Molnar, K., Laszlo, L., 2014. Intracellular processing of disease-associated alpha-synuclein in the human brain suggests prion-like cell-to-cell spread. Neurobiol. Dis. 69, 76–92.

Madisen, L., Mao, T., Koch, H., Zhuo, J.M., Berenyi, A., Fujisawa, S., Hsu, Y.W., Garcia 3rd, A.J., Gu, X., Zanella, S., Kidney, J., Gu, H., Mao, Y., Hooks, B.M., Boyden, E.S., Buzsaki, G., Ramirez, J.M., Jones, A.R., Svoboda, K., Han, X., Turner, E.E., Zeng, H., 2012. A toolbox of Cre-dependent optogenetic transgenic mice for light-induced activation and silencing. Nat. Neurosci. 15, 793–802.

Mandel, R.J., Marmion, D.J., Kirik, D., Chu, Y., Heindel, C., McCown, T., Gray, S.J., Kordower, J.H., 2017. Novel oligodendroglial alpha synuclein viral vector models of multiple system atrophy: studies in rodents and nonhuman primates. Acta Neuropathol Commun. 5, 47.

Michalski, J.P., Anderson, C., Beauvais, A., De Repentigny, Y., Kothary, R., 2011. The

proteolipid protein promoter drives expression outside of the oligodendrocyte lineage during embryonic and early postnatal development. PLoS One 6, e19772.
Muzumdar, M.D., Tasic, B., Miyamichi, K., Li, L., Luo, L., 2007. A global double-fluorescent Cre reporter mouse. Genesis. 45, 593–605.
Nakazato, Y., Yamazaki, H., Hirato, J., Ishida, Y., Yamaguchi, H., 1990. Oligodendroglial microtubular tangles in Olivopontocerebellar atrophy. J. Neuropathol. Exp. Neurol. 49, 521–530.
Papp, M.I., Kahn, J.E., Lantos, P.L., 1989. Glial cytoplasmic inclusions in the CNS of patients with multiple system atrophy (striatonigral degeneration, olivopontocerebellar atrophy and Shy-Drager syndrome). J. Neurol. Sci. 94, 79–100.
Parkkinen, L., Hartikainen, P., Alafuzoff, I., 2007. Abundant glial alpha-synuclein pathology in a case without overt clinical symptoms. Clin. Neuropathol. 26, 276–283.
Rodriguez-Diehl, R., Rey, M.J., Gironell, A., Martinez-Saez, E., Ferrer, I., Sanchez-Valle, R., Jague, J., Nos, C., Gelpi, E., 2012. "Preclinical" MSA in definite Creutzfeldt-Jakob disease. Neuropathology. 32, 158–163.
Shults, C.W., Rockenstein, E., Crews, L., Adame, A., Mante, M., Larrea, G., Hashimoto, M., Song, D., Iwatsubo, T., Tsuboi, K., Masliah, E., 2005. Neurological and neurodegenerative alterations in a transgenic mouse model expressing human alpha-synuclein under oligodendrocyte promoter: implications for multiple system atrophy. J. Neurosci. 25, 10689–10699.
Soriano, P., 1999. Generalized lacZ expression with the ROSA26 Cre reporter strain. Nat. Genet. 21, 70–71.
Spillantini, M.G., Schmidt, M.L., Lee, V.M., Trojanowski, J.Q., Jakes, R., Goedert, M., 1997. Alpha-synuclein in Lewy bodies. Nature. 388, 839–840.
Spillantini, M.G., Crowther, R.A., Jakes, R., Cairns, N.J., Lantos, P.L., Goedert, M., 1998. Filamentous alpha-synuclein inclusions link multiple system atrophy with Parkinson's disease and dementia with Lewy bodies. Neurosci. Lett. 251, 205–208.
Stefanova, N., Wenning, G.K., 2015. Animal models of multiple system atrophy. Clin. Auton. Res. 25, 9–17.
Tanji, K., Mori, F., Mimura, J., Itoh, K., Kakita, A., Takahashi, H., Wakabayashi, K., 2010. Proteinase K-resistant alpha-synuclein is deposited in presynapses in human Lewy body disease and A53T alpha-synuclein transgenic mice. Acta Neuropathol. 120, 145–154.
Tu, P.H., Galvin, J.E., Baba, M., Giasson, B., Tomita, T., Leight, S., Nakajo, S., Iwatsubo, T., Trojanowski, J.Q., Lee, V.M., 1998. Glial cytoplasmic inclusions in white matter oligodendrocytes of multiple system atrophy brains contain insoluble alpha-synuclein. Ann. Neurol. 44, 415–422.
Wakabayashi, K., Matsumoto, K., Takayama, K., Yoshimoto, M., Takahashi, H., 1997. NACP, a presynaptic protein, immunoreactivity in Lewy bodies in Parkinson's disease. Neurosci. Lett. 239, 45–48.
Wenning, G.K., Geser, F., Krismer, F., Seppi, K., Duerr, S., Boesch, S., Kollensperger, M., Goebel, G., Pfeiffer, K.P., Barone, P., Pellecchia, M.T., Quinn, N.P., Koukouni, V., Fowler, C.J., Schrag, A., Mathias, C.J., Giladi, N., Gurevich, T., Dupont, E., Ostergaard, K., Nilsson, C.F., Widner, H., Oertel, W., Eggert, K.M., Albanese, A., del Sorbo, F., Tolosa, E., Cardozo, A., Deuschl, G., Hellriegel, H., Klockgether, T., Dodel, R., Sampaio, C., Coelho, M., Djaldetti, R., Melamed, E., Gasser, T., Kamm, C., Meco, G., Colosimo, C., Rascol, O., Meissner, W.G., Tison, F., Poewe, W., 2013. The natural history of multiple system atrophy: a prospective European cohort study. Lancet Neurol. 12, 264–274.
Yazawa, I., Giasson, B.I., Sasaki, R., Zhang, B., Joyce, S., Uryu, K., Trojanowski, J.Q., Lee, V.M., 2005. Mouse model of multiple system atrophy alpha-synuclein expression in oligodendrocytes causes glial and neuronal degeneration. Neuron. 45, 847–859.
Zhang, L., Cao, B., Zou, Y., Wei, Q.Q., Ou, R., Liu, W., Zhao, B., Yang, J., Wu, Y., Shang, H., 2018. Causes of death in Chinese patients with multiple system atrophy. Aging Dis. 9, 102–108.
Zong, H., Espinosa, J.S., Su, H.H., Muzumdar, M.D., Luo, L., 2005. Mosaic analysis with double markers in mice. Cell. 121, 479–492.